Study of flashover in full-scale room fires using imaging technologies

Mozaffari, M. Hamed; Li, Yuchuan; Weinfurter, Mark; Ko, Yoon

https://doi.org/10.4224/40003413

NRC·CNRC CONSTRUCTION

Study of flashover in full-scale room fires using imaging technologies

M. Hamed Mozaffari, Yuchuan Li, Mark Weinfurter, Yoon Ko

Report no.: A1-020368
Report date: 11 Sep 2024

National Research Council Canada
Conseil national de recherches Canada

Canada

GC Catalogue: NR24-127/2024E-PDF
ISBN: 978-0-660-73576-4

Study of room fire flashover in full-scale tests using imaging technologies

Author

MozaffariMaaref.MohammadHamed
Digitally signed by MozaffariMaaref, MohammadHamed
DN: cn=MozaffariMaaref, MohammadHamed, c=CA, o=GC, ou=NRC-CNRC, email=mhamed.mozaffarimaaref@cnrc-nrc.gc.ca
Date: 2024.09.11 15:06:58 -04'00'

M. Hamed Mozaffari

Approved

Kashef, AH
9/20/24 05:11

Ahmed Kashef, PhD
Program Leader
Fire Safety R&D
NRC Construction Research Centre

Report no.: A1-018587.2
Report date: August 6, 2024
Program: Fire Safety R&D

Copy no. 1 of 1

Table of Contents

List of Figures

List of Tables

Study of room fire flashover in full-scale tests using imaging technologies

Authors: M. Hamed Mozaffari, Yuchuan Li, Mark Weinfurter, Yoon Ko

Executive summary

This report presents findings from seven full-scale room fire test experiments undertaken at the Fire Safety Unit (SFU) of the National Research Council Canada (NRCC). The primary objective of this set of tests was to gather data for use in the analysis of room fire dynamics, with a specific focus on the analysis, detection and prediction of the flashover phenomenon. Briefly, flashover is the last indication for a building to be tenable, which means that after that (post-flashover), it is almost impossible for tenants to be alive in the room. The time window from ignition to flashover is typically about five minutes, underscoring the urgency in predicting this event to enhance both civilian and firefighter safety.

Imaging technologies have emerged with significant potential to assist in pattern recognition in various applications, including fire safety. Coupled with AI, image technologies can be utilized to assist in the detection and prediction of flashover in room fire incidences and rescues [1], [2], [3], [4]. However, a major challenge in applying these new technologies in this context is a lack of understanding of the technologies and their image data. This report addresses this gap by providing an extensive experimental investigation into the image data collected from controlled room fire tests conducted under varied conditions. We utilized many instruments, including different types of thermal infrared cameras, RGB cameras, sensors (temperature, heat flux gauges, and pressure), acoustic imaging devices, gas analyzers and more. The data obtained from these devices are discussed for room fire dynamics, which are related to the room size specifications, fuel amount, opening area for oxygen and so on.

In this project, seven full-scale room fire tests were designed using pre-estimated calculations (e.g., heat release rate, fuel amount, opening area size, etc.) to produce various room fire dynamics, including flashover and no flashover. A total of 1.8 terabytes of data were captured using an array of instruments, including thermal infrared cameras, RGB cameras, temperature sensors, heat flux gauges, pressure sensors, an acoustic imaging device and a gas analyzer.

This dataset not only serves the immediate goals of this study but also provides a valuable resource for further research. Future applications and use cases of this dataset include:

1- It is possible to compare imaging technologies, such as different thermal infrared cameras.
2- Further training and validation of AI techniques for fire safety, such as flashover prediction, is now possible using actual room fire test data.
3- The dataset provides valuable room fire data for further study of flashover behavior in room fires using other advanced technologies, such as pressure sensors and acoustic imaging.
4- Vision-based data collected provide researchers with access to validation data for vision-based modeling and simulation of room fire dynamics.
5- It is now possible to select the best vision-based data acquisition technique in future room fire tests for the advancement of vision-based flashover detection and prediction techniques.
6- The dataset provides invaluable vision-based data to be used in the development of emerging digital technologies, such as the Internet of Things (IoT), smart firefighter robots and smart detectors.
7- Comparison between the performance of common fire-related sensors versus imaging technologies becomes possible for the detection, monitoring and prediction of flashovers and other fire hazards.

This report enhances the understanding of room flashover dynamics and contributes to the development of innovative fire safety measures and technologies.

Results from this project were also utilized in the validation of our in-house user calibration of a mid-infrared cooled thermal camera that was performed concurrently (more details can be found in Section 2.5.2).

1 Introduction

1.1 Background

Flashover is known to be the most serious and fatal fire dynamic in room fire incidents. The ISO 13943 standard [5] defines flashover as the onset of the rapid transition in the state of the fire, whereby the total surface of combustible materials start to burn simultaneously, and the flame spreads throughout the entire room. The main driving force of flashover is the heat radiated from the hot smoke layer rapidly accumulating near the ceiling, which heats the exposed surface of all the items in the room. Subsequently, the rapid temperature rise on the surface of the combustible contents produces hot pyrolysis gases and ignites them [6]. Figure 1 presents a time progression of a test compartmental fire. As presented in the figure, for a standard-size room with a closet, carpet and bed, flashover onset occurs within five minutes. Flashover could also cause the fire to spread to other compartments or nearby structures, which would endanger all the occupants and firefighters in the building.

Figure 1. The rapid growth of fire in a test room with modern upholsteries. From left to right, it takes less than five minutes from ignition to flashover onset.

To save the lives of occupants and firefighters, much research has focused on identifying the signs of impending flashover and predicting the onset. They found that the occurrence of flashover depends on several factors [7], [8], [9] including, but not exclusive to, fire growth rate, ventilation opening area, wall and ceiling material, room dimensions and room temperature. To understand the likelihood of flashover in relation to these factors, statistical analyses of a naturally ventilated compartment fire were studied [10], and Monte Carlo (MC) simulations were also carried out [11]. These studies [9], [10], [11] indicated that the vent opening width is one of the most important factors affecting the probability of flashover onset. Other studies showed that even wind [12] and the wall's heat transfer rate [13] could affect the probability and timing of flashover.

While there are many factors affecting flashover onset, flashover criteria are suggested based on temperature, ventilation size and heat release rate used by many researchers [14], [15], [16]. Consensus criteria are that for a typical room fire, the onset of flashover corresponds to the time when the upper smoke layer in the room reaches a temperature of around 600˚C. Also, at the time of flashover occurrence, the heat flux (HF) from the upper smoke layer reaches approximately 20 kW/m^2 when measured "on the floor." In addition, the onset of flashover can be estimated by monitoring the growth of the heat release rate (HRR). While varying with the room, door and window size, the average HRR value needed for flashover occurrence is 1000 kW - 2000 kW for a typical small room, similar to the standard room described in ISO 9705: 1993 standard [15], with one open doorway.

1.2 Problem

Applying the room flashover criteria to the fire ground is not straightforward since room temperature, HF and HRR are often unknown in an actual fire, so many firefighters rely upon their judgment or experience in recognizing visual indicators of room flashover.

Visual indicators of flashover have been investigated so far in multiple studies [17], [18], [19], [20]. From many experimental room fire tests in the literature, and specifically from Francis and Chen [17], the visual indicator of flashover is confirmed as the observation of "extrusive flame" crossing the header of a door or window and projecting beyond the vent.

It is noted that there are five categories of compartment fire that evolve beyond smoldering but rely on unpressurized contained fuel [17]. These fire categories exist ranging from fuel-restricted pre-flashover fires at one extreme, to vent-restricted pre-flashover fires at the other. In the middle, there are three categories of post-flashover fires where neither fuel nor vent restriction is sufficient to prevent flashover. Understanding these categories can enhance firefighter training and

preparedness by providing clearer expectations about the behavior of fires under different conditions.

Further studies are necessary since these studies used simulated image data and reduced-scale room fire test image data. A large number of image data from full-scale room fires are needed to be used in the analyses of visual indicators of flashover, which will help not only detect but also predict room flashover.

1.3 Objectives

With the long-term goals of developing an automatic method using artificial intelligence to detect and predicting flashover in real time using visual data captured from full-scale room fires, the Fire Safety Unit (FSU) of the Construction Research Center (CRC) at National Research Council Canada (NRC) has initiated a Vision-based Smart Firefighting Tool Development (VSFTD) project.

In Phase 1 of the VSFTD project, a comprehensive literature review was conducted on common flashover detection and prediction methods. The review covered all methods of flashover analysis, including conventional techniques relying on recorded data from sensors and gauges, synthetic/CFD simulated data and the application of novel machine learning and vision-based methods. A gap identified by the literature review is that there is a limited number of actual vision-based datasets with a quality good enough for studying flashover phenomena in full-size room fires.

This report discusses hase 2 of the VSFTD project, where a series of full-scale room fire tests was conducted to systematically acquire a large number of the image/video data of the room fires using various imagers. These data will be used in future for the development of advanced image processing techniques and to develop vision-based modules to process real-time images of fire and smoke to detect and predict room flashover. This report describes and compiles the results of seven full-scale room fire experiments conducted.

A series of tests under Phase 2 of the VSFTD project were conducted to address the following needs of the project:

- Collect the image/video data of full-scale room fires using different imaging technologies. These data will be used for the development of artificial intelligence and vision-based flashover detection and prediction methods.

- Link and compare the image/video data with the sensor data for validation of vision-based methods and various imaging technologies.
- Allow researchers to study room fires with different room configurations regarding opening, door size and fuel amounts.
- Compare the output images from different imaging technologies to understand the performance of each one in capturing smoke and flame development in a room.

2 Experiment test setup

2.1 Test room

To collect a big dataset of full-scale compartment fires, we designed and built a full-scale compartment, the dimensions of which were approximately 2.4 m (L) × 3.6 m (W) × 2.4 m (H), similar to those of the ISO 9705 test room [21]. Figure 2 presents examples of the opening with the modified sizes used in our test experiments. Figure 3 shows the details of our standard test room with a modifiable doorway/window. Details of each room fire test experiment are provided in Table 1 as well as Figure 4 and Figure 5.

Figure 2. Examples of openings with different sizes used in our room fire test experiments

2.2 Fires

A wood crib with a different number of layers was used as the fuel in each test. The details of the wood crib are:

- The wood crib was made with kiln-dried (KD-HT), spruce-pine-fir (S-P-F) lumber pieces.
- Each lumber piece measured 38 mm x 89 mm x 800 mm.

- The pieces were evenly spaced in rows based on the purpose of the experiment as per the test plan.
- The wood pieces were stacked (with upright 38 mm x 89 mm rectangular cross sections) in parallel pairs at right angles to the parallel pair immediately below to heights (e.g., 712 mm (eight rows high) or ~ 1068 mm (12 rows high)). See Figure 5 as an example of eight rows or six rows.

The wood crib was placed on concrete blocks, 102 mm higher than the surface of the room floor. The wood crib was ignited from underneath with 1000 mL of methanol (density 796 kg/m^3, heat of combustion 20 MJ/kg), which was distributed equally among five shallow metal pans (200 mL per pan) having a mean diameter of 18.5 mm. The total heat output of this ignition source is at least 40 kW, and the free-burning time could be about 360s.

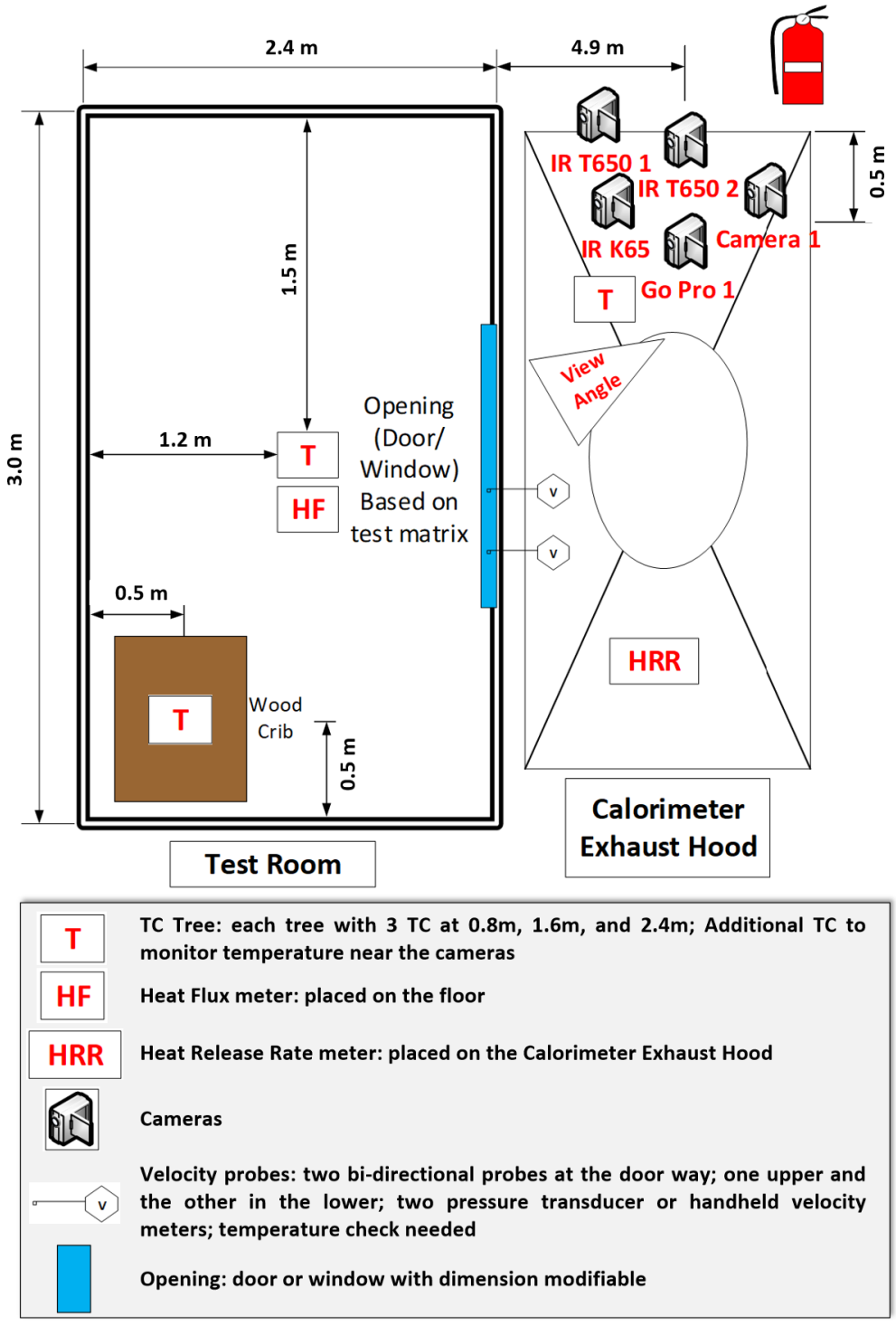

Figure 3. Details of test room built for recording visual and sensor data for study flashover

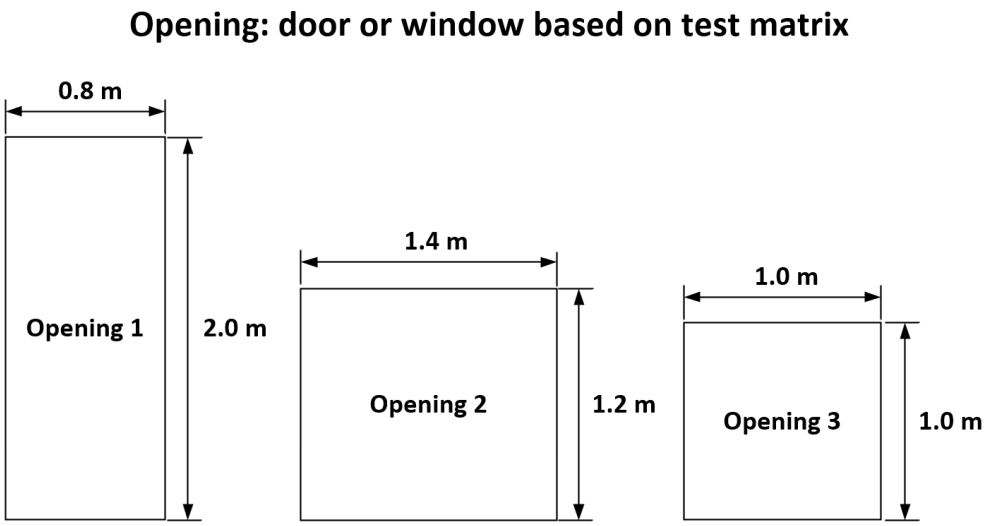

Figure 4. Illustration of the dimensions of openings in our room fire test experiments

Figure 5. Example of wood cribs as the fuel source used in our room fire tests. Measurements were accurate as possible for each experiment.

2.3 Test matrix

The experiments were planned to have many of the types of room fires categorized by Francis and Chen [17], such that the test room could experience compartment fires of fuel-restricted pre-flashover fire (no flashover), post-flashover fire with varying fire growth rates and flashover onsets. In designing the fires, the HRR at flashover was calculated based on Babrauskas [22] and Thomas [23], and the room configuration/opening size, as well as the layers of the wood crib, were planned to generate the designed room fires. The calculation equations of Babrauskas [22] and Thomas [23] are presented in Appendix A.

Seven room fire tests were planned to investigate flashover and no-flashover cases. The parameters of the fuel, window/door size, the purpose of each experiment as well as pre-estimation of HRR at flashover are tabulated in Table 1.

Table 1. Details of test matrix used in room fire test experiments

Exp #	Opening size		Wood cribs		Flashover estimation	Estimated $\dot{Q}_{FO}$	
	Width (m)	Height (m)	# Layers	Weight (kg)		Babrauska [22] (kW)	Thomas [23] (kW)
Test 1	0.8	2.0	8	67	Fast onset	1697	1157
Test 2	0.8	2.0	4	33	No flashover	-	-
Test 3	1.4	1.2	8	67	Fast onset	1380	997
Test 4	1.4	1.2	9	96	Fast onset	1380	997
Test 5	1.0	1.0	8	67	Relaxed onset	750	685
Test 6	1.0	1.0	6	52	Relaxed onset	750	685
Test 7	1.0	1.0	4	31	No flashover	-	-

2.4 Instrumentation

The test room was instrumented to collect thermal data using common thermocouple sensors. While the main goal of the experiment was to record image-based data using RGB and thermal infrared cameras, the sensor data was needed for characterizing the room fire and collected image data corresponding to the thermal condition evolved in the test room. The thermal sensor data were also used for the validation of the visual signatures collected for smoke and flame development in the test room. Therefore, the test room was instrumented with thermocouples, a heat flux gauge, and velocity probes, as well as for HRR. The measurements of heat flux, room temperature and HRR were analyzed for the main criteria for flashover onset.

The test room was built under a calorimetry hood system capable of measuring the HRR of the test room with the duct smoke temperature, flow rate and concentrations of oxygen, carbon monoxide and carbon dioxide. The exhaust duct and the data acquisition system to measure the HRR are shown in Figure 6.

In the test room, as shown in Figure 7, a thermocouple tree with three temperature measurements at equal distances from the bottom of the test room to record temperatures at different heights (0.6 m, 1.6 m, 2.4 m) was placed. The thermocouple tree was placed away from the wood crib to measure the room temperature in tests #1 – #4, while it was placed at the wood crib to measure the fire temperature in tests #5 – #7. At the centre of the room on the floor, a heat flux gauge, as shown in Figure 8, was installed to record the radiative heat emitted from the ceiling smoke layer in the test room. The heat flux gauge was connected to a water-cooling system to ensure measurement accuracy. To monitor the air flows via the opening, a velocity probe was installed on the top and bottom of the opening, as shown in Figure 9, and each of these probes was connected to a pressure transducer. Figure 10 shows the support systems of the water-cooling system for the heat flux gauge and pressure transducers for the velocity probes.

Figure 6. The exhaust duct used in our experiments capable of measuring HRR

Figure 7. Tree thermocouple used in our room fire test experiments

Figure 8. Heat flux gauge installed on the floor of the room fire test

Figure 9. Gas flow pressure sensors installed on the top and bottom of openings

Figure 10. Support systems installed at the back of the room for heat flux and pressure gauges

2.5 Imaging devices and thermal infrared cameras

This project was unique in employing all types of image-based devices. In general, there were two types of thermal infrared cameras in use today, and this study tested both types: high-performance cooled photon-counting and uncooled microbolometer-based thermal IR camera. Five high-end thermal infrared cameras were used in these room fire tests:

- Two long-wave warm detector cameras (microbolometer-based FLIR T650sc);
- One mid-wave cold detector camera (cooled photon-counting FLIR A8303sc);
- One firefighting-grade handheld thermal camera (microbolometer-based FLIR K65).

Also, five RGB cameras were installed to record the development of fire from different view angles in each experiment:

- Two different RGB cameras (Go Pro SJ6000 (MOV format));
- Canon VIXIA HF R50 (MP4 format) fixed at a distance from the room and viewing opening area;
- Mobile phone (iPhone X);
- Olympus professional DSLR camera used to record fire growth from other view angles (e.g., side view and in action view).

Table 2 illustrates the main thermal IR cameras that were used in this project for recording IR videos from each room fire tests.

Table 2. Main thermal cameras utilized in this project

Name	FLIR T650sc	FLIR A8303sc	FLIR K65
configuration	Long-wave IR uncooled microbolometer-based detector 7.5 to 13.0 µm	Mid-wave IR cooled detector using Indium Antimonide (InSb) detector that operates in the 3.0 to 5.0 µm waveband	Firefighting IR uncooled microbolometer-based detector 8 to 14 µm
Image			

Brief details regarding camera capabilities	- Records data with three fixed temperature ranges from low -40˚C to high 2000˚C - Connected to PC to record raw data on PC - Continuous automatic and manual focus ranges - High resolution 640 by 480 pixels - Variable frame rates up to 30 Hz - RGB camera and Multi-spectral dynamic imaging (MSX) technology - Various lenses and filters	- Records data using factory-based and user-based calibrations with temperature ranges up to 3000˚C - Connected to PC to record raw data on PC - Super-resolution 1280 by 720 pixels - Continuous manual focus ranges - High frame rate of up to 60 Hz full frame - Various lenses and filters	- Records data from -20˚C to 650˚C in two temperature modes - Records data on memory only - Resolution 320 by 240 pixels - Fixed focus - TI Basic NFPA fire-fighting mode - Special isotherm (colourmap) according to NFPA - Frame rate up to 60 Hz, Non-radiometric IR video recording

For the RGB and IR cameras, a mounting fixture was newly designed and built to allow similar view angles towards the test room. It was placed outside the test room, as shown in Figure 3 and Figure 11. It is noteworthy to mention that based on the opening size in each test, we changed the orientation of the cameras to record the maximum amount of information.

2.5.1 Data acquisition computer systems

The output data from all cameras were recorded and saved during the test. For the two T650sc and A8303sc IR cameras, two tower PCs were used for the output video data acquisition and recording. For the data acquisition, two software tools, FLIR ResearchIR and FLIR Research Studio, were used. Figure 11 illustrates the experimental setup of the data acquisition computer systems and our cameras mounted on our designed fixture. In order to protect the cameras from the radiative heat from smoke and flame, we installed a thermocouple over the main cameras, and the temperature was monitored in each test (see Figure 12).

2.5.2 Calibration

Unlike the RGB cameras used in the tests, the IR cameras need to be calibrated for measurement accuracy. The calibration should be completed considering the target, the surrounding thermal conditions, as well as the quality and technology of the camera components, such as the detector, lens and recording technique. Therefore, some cameras have features to allow user calibration where factory calibration is not suitable. High-end cameras usually used for research, such as FLIR A8303sc, which we used in this study, provide the possibility of performing user-calibration based on the application. For the application to study flame and smoke development in a room, we carried out user calibrations with the FLIR A8303sc with extensive research and experiments prior to the room fire tests. Thus, in this study, the FLIR A8303sc camera was user-calibrated for the temperature range span from low 40˚C to high 1200˚C, corresponding to general room fire

temperatures. The complete user calibration procedures and validation test results are available in a complementary report [24].

2.6 Other advanced devices

Besides the sensors and vision-based cameras mentioned in previous sections, we also explored other devices to collect more data relevant to the room fire:

- A FLIR thermometer gun (Figure 13) with a temperature measurement range of 2000˚C, which was used to monitor the temperature near the ceiling of the test room.
- An acoustic imaging camera (FLIR si124), which was explored for potential applications to fire-related information collection. The ultrasonic and vision-based detection camera is usually used for locating pressurized leaks in compressed air systems or detecting partial discharge from high-voltage electrical systems [25]. We used this acoustic imaging camera to record data for the first time in flashover phenomena. This device has 124 microphones to locate the source of noise in the environment. Figure 14 shows this new technology used in our room fire test experiments.
- A miniature thermal IR lens (FLIR One) that has a temperature range of up to 400˚C with resolution of 160 by 120 pixels (see Figure 15). We used this camera to know its performance in fire situations in comparison to other cameras. In addition to all those cameras explained so far, we recorded videos from the side face of the room opening to record RGB videos when flame and smoke rush out from the opening from a side view angle.

Figure 11. Mounting setup of cameras and tower PCs for recording data

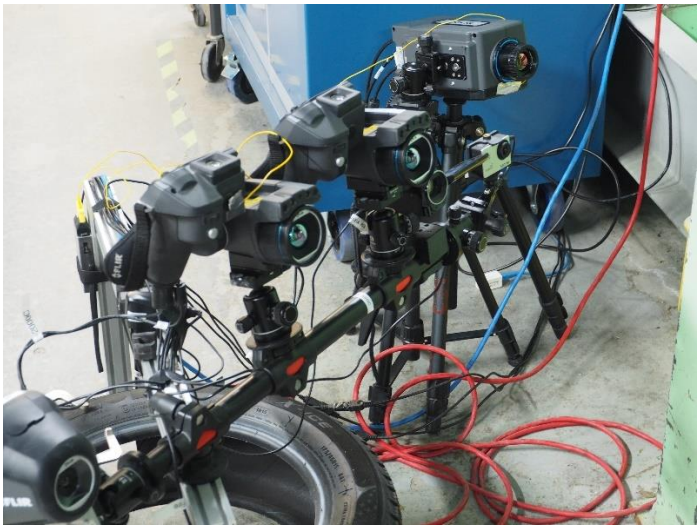

Figure 12. Thermocouples installed for monitoring of temperature around camera lenses

Figure 13. Vision-based thermometer gun equipped with two IR lasers

Figure 14. FLIR si124 acoustic imaging camera used in our tests

Figure 15. FLIR one pro camera connected to Samsung S22 Ultra smart phone

3 Test sensor data

Along with the image data collected by the cameras, sensor data were collected for room temperature, heat flux and HRR, which were used to verify/characterize the image data collected using the IR cameras and vision cameras corresponding to the thermal conditions in the test room. The measured HRR, heat flux and temperature data from each test are plotted in Figure 16 to Figure 22.

These sensor data were used for linking the image data with the room fire development, in particular for pre-flashover and post-flashover. The onset of flashover was thus determined based on these test sensor data of HRR, heat flux and temperature, which are generally used as the main criteria for flashover occurrence. Following the criteria for a typical room to detect the onset of flashover (i.e., heat flux of 20-25 KW/m^2 on the floor, ceiling smoke layer temperature of approximately 600˚C, as well as HRR at the flashover onset based on the room/ventilation conditions), the onset in each test was determined. It should be noted that for tests #5, #6 and #7 the onset was determined mainly on the HRR and heat flux since the thermocouple tree was placed at the wood crib to measure flame temperature rather than the room/ceiling layer temperature.

Table 3 shows the flashover onset and the HRR at the onset of each test. As the amount of fuel and opening size were designed to result in different room fire types, the flashover onset in each test varies accordingly: fast onset resulted in tests #1, #3 and #4; relaxed onset resulted in tests #5 and #6; and no flashover resulted in tests #2 and #7.

Linking the recorded image frames to the flashover occurrence based on the sensor data, visual flashover indicators in the recorded RGB data were monitored. One of the indicators was the appearance of flame in the smoke region outside of the opening area, which was more apparent in the RGB data than the IR data. On the other hand, the recorded IR data visualized the distinct ceiling smoke layer as an indicator for flashover with the elevated temperature close to 600˚C at the time of flashover.

Table 3. Flashover onset and the measured HRR at the onset. Measured $\dot{Q}_{FO}$ is calculated based on the equation in Appendix B.

Exp #	Opening size		Wood cribs	Flashover		Measured$\dot{Q}_{FO}$[1]
	Width (m)	Height (m)	# Layers	Based on HF/HRR/TC		(kW)
Test #1	0.8	2.0	8	182s after ignition	Fast onset	1036
Test #2	0.8	2.0	4	No flashover	No flashover	-
Test #3	1.4	1.2	8	201s after ignition	Fast onset	1115
Test #4	1.4	1.2	9	190s after ignition	Fast onset	1024
Test #5	1.0	1.0	8	297s after ignition	Relaxed onset	919
Test #6	1.0	1.0	6	242s after ignition	Relaxed onset	843
Test #7	1.0	1.0	4	No flashover	No flashover	-

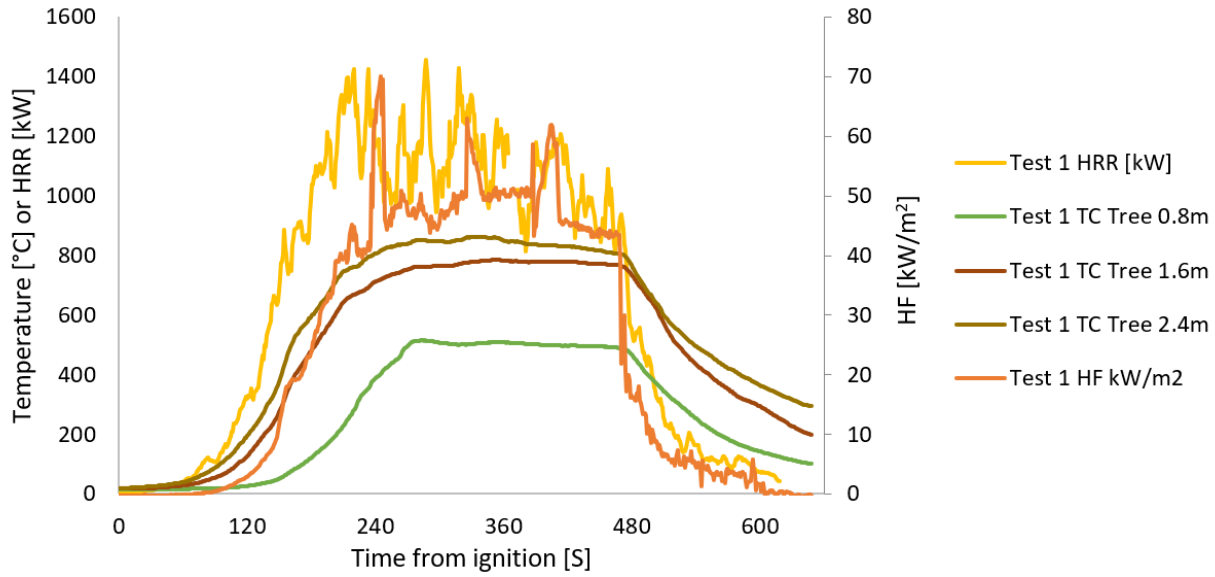

Figure 16. Comparison between sensor data in Test #1. The flashover onset was determined at 182 seconds after the fire was ignited. The thermocouple tree was located far from the wood cribs in the corner of the room.

[1] Measured $\dot{Q}_{FO}$ was calculated based on the equation in Appendix B.

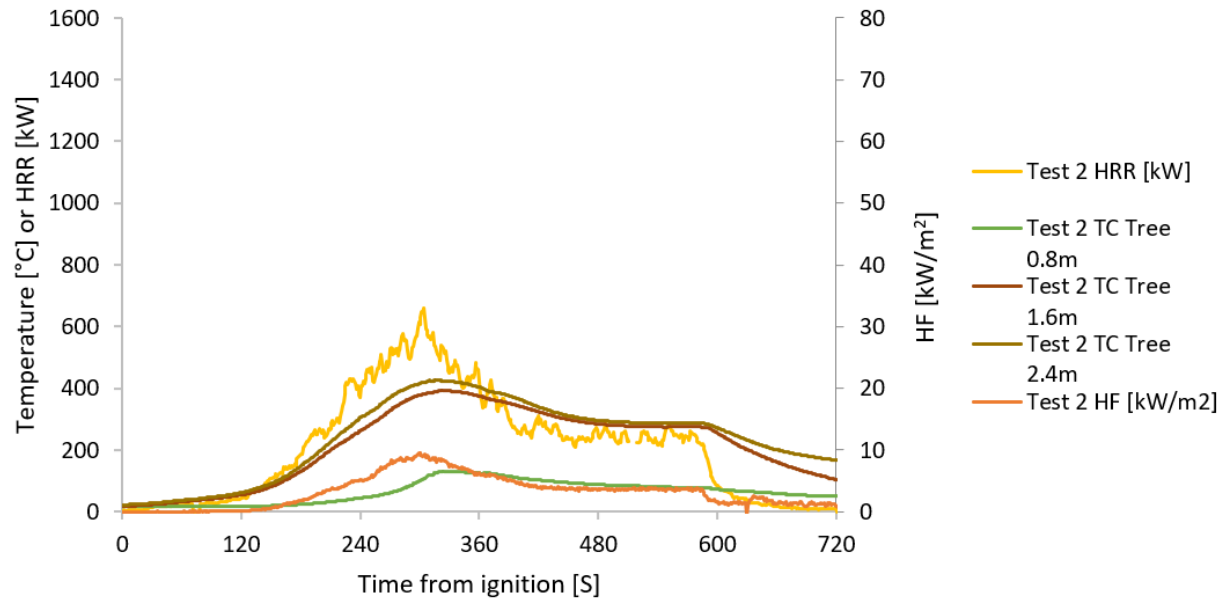

Figure 17. Comparison between sensor data in Test #2. No flashover was observed in this test. The thermocouple tree was located far from the wood cribs in the corner of the room.

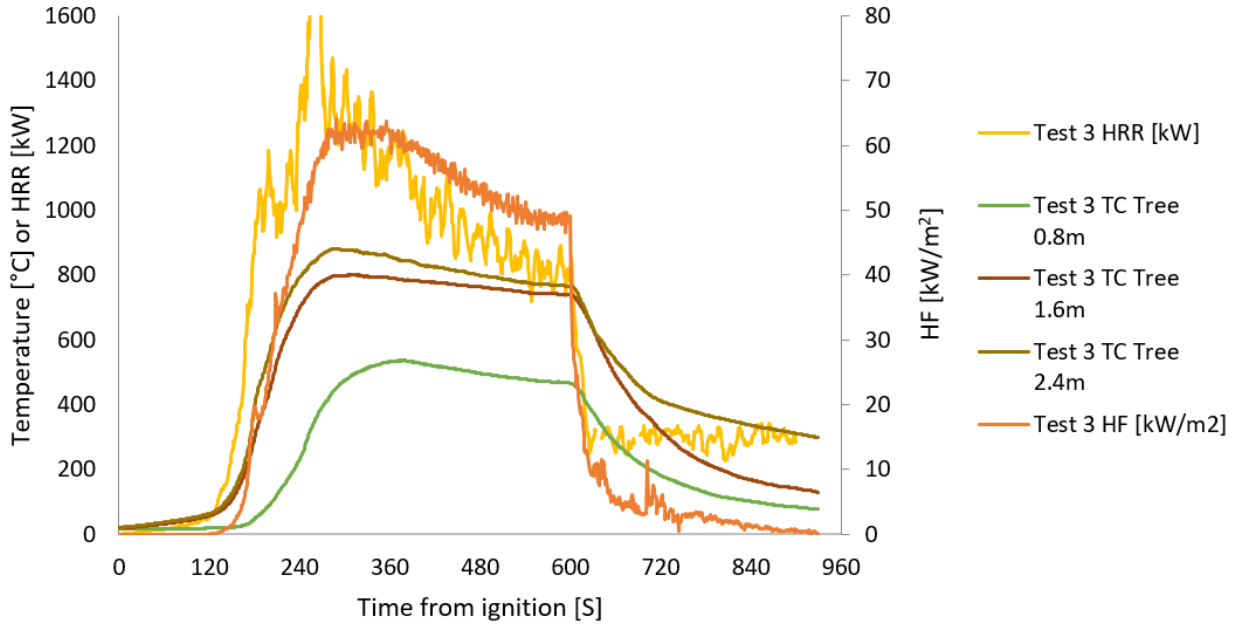

Figure 18. Comparison between sensor data in Test #3. The flashover onset was determined at 201 seconds after the fire was ignited. The thermocouple tree was located far from the wood cribs in the corner of the room.

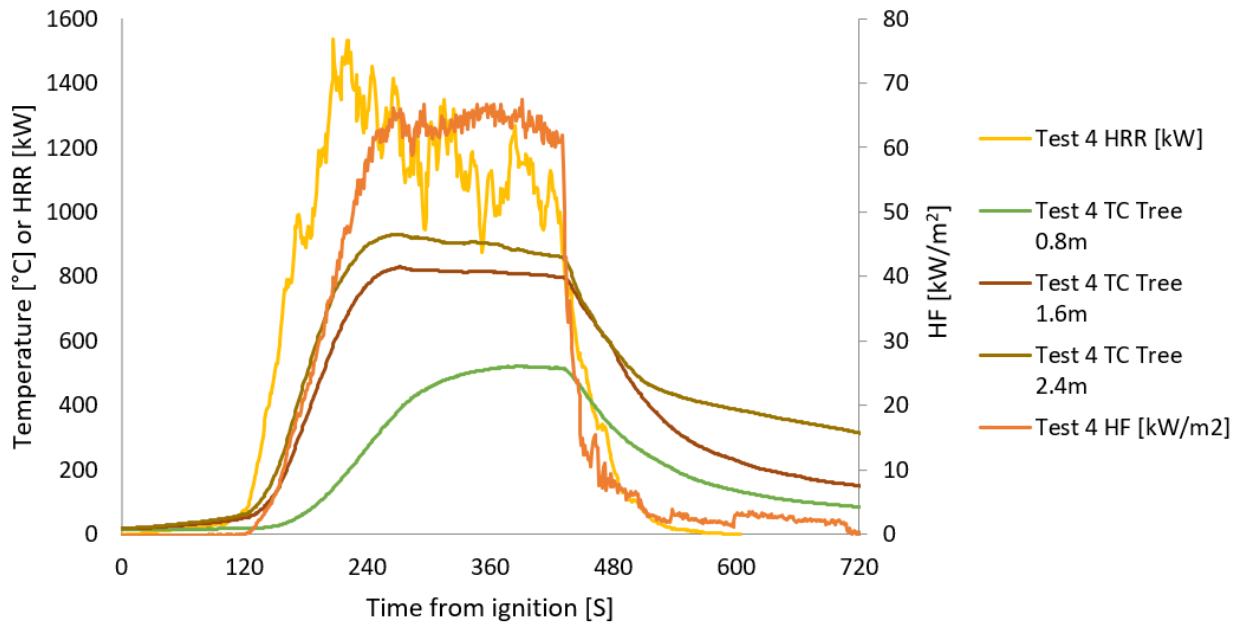

Figure 19. Comparison between sensors data in Test #4. Flashover onset was determined at the time 190s after the ignition of the fire. The thermocouple tree was located far from the wood cribs in the corner of the room.

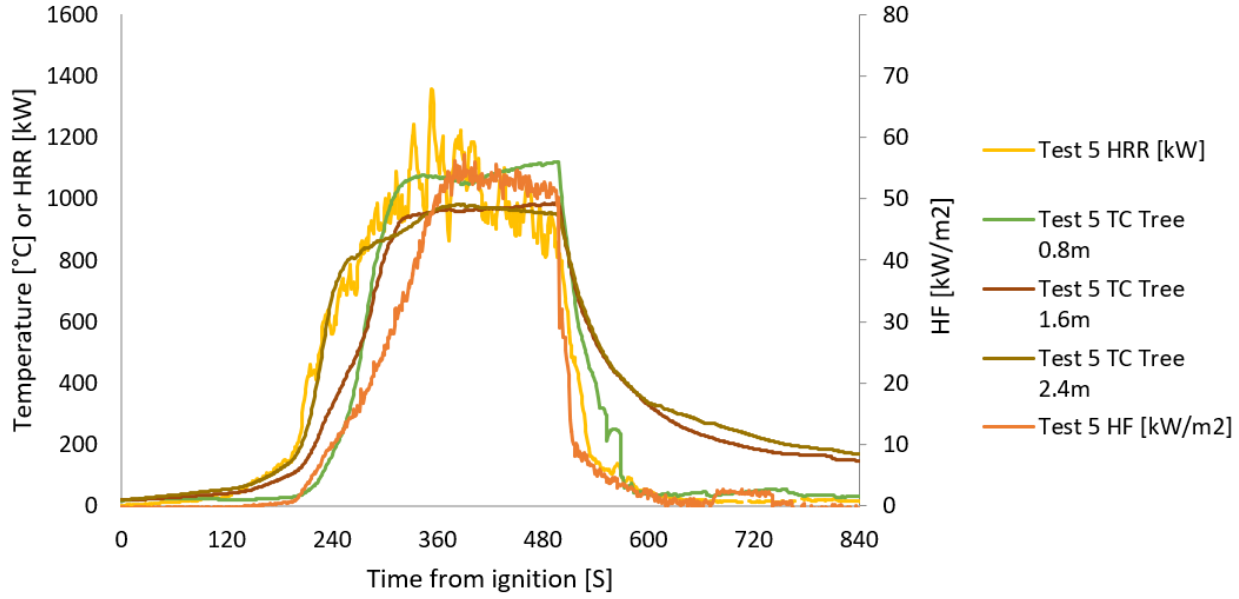

Figure 20. Comparison between sensor data in Test #5. The flashover onset was determined at 297 seconds after the fire was ignited. The thermocouple tree was located between the wood cribs. Therefore, the temperature was not valid for this experiment.

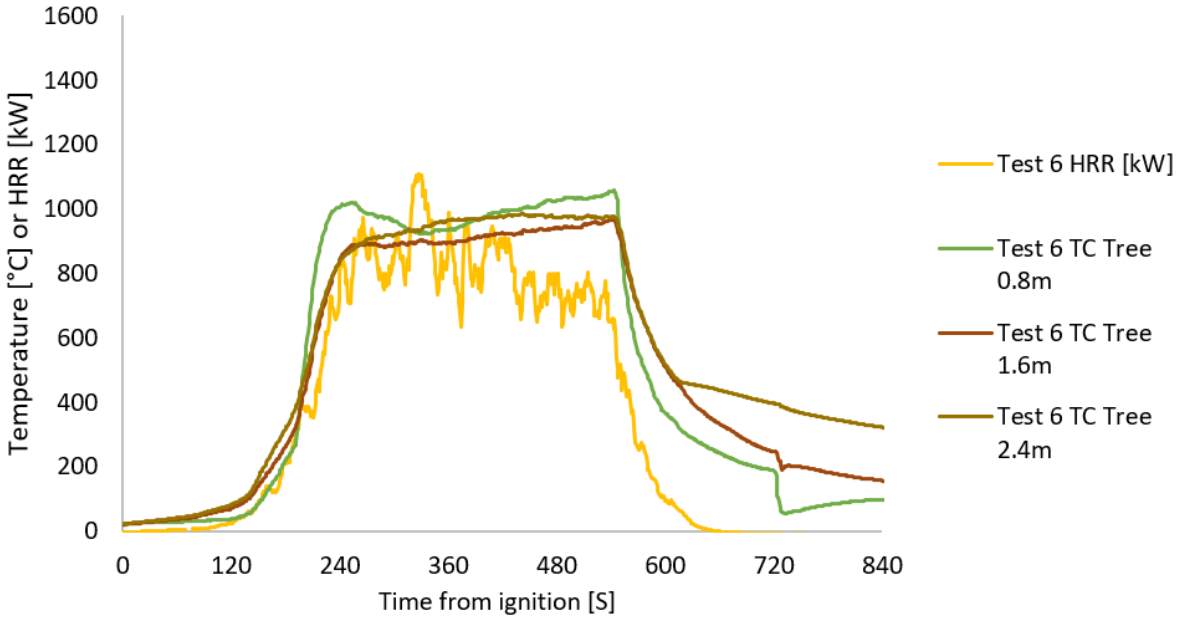

Figure 21. Comparison between sensor data in Test #6. The flashover onset was determined at 240 seconds after the fire was ignited. The thermocouple tree was located between the wood cribs. HF data was deleted here due to a malfunctioning gauge.

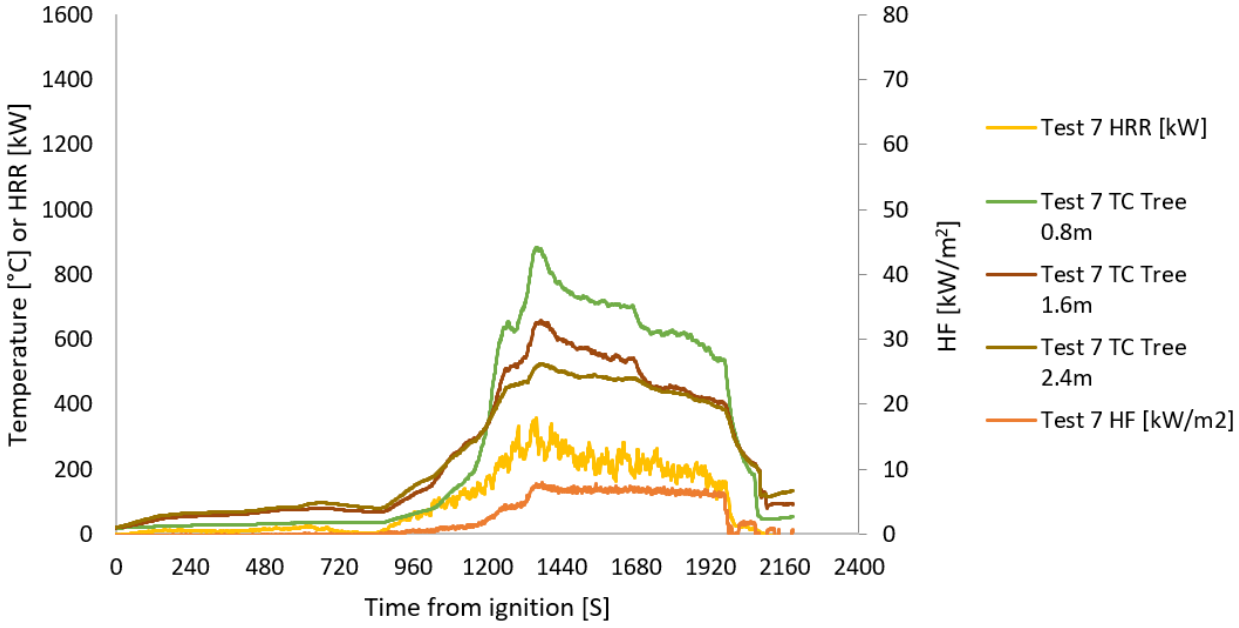

Figure 22. Comparison between sensors data in Test #7. There was no flashover observed in this experiment. Thermocouple tree was located far from the wood cribs in the corner of the room.

4 Image data acquisition and comparison of imaging devices

This section describes the image data acquisition and compares the output image data from the different cameras used in this project.

4.1 Image data acquisition to study room fires

To enable the image data acquisition and cross-comparisons between all vision RGB and thermal IR image data, we set the settings on all the cameras to be as similarly as possible. All the cameras were placed for a similar view angle toward the fire room. The start and end of each test were marked using a wood slab as a clapperboard, for easy data processing and synchronization with other sensor data (e.g., thermocouples, heat flux gauge, HRR, etc.).

FLIR ResearchIR and FLIR Research Studio are two pieces of software that were used for recording raw data with *.ats or *.seq output formats. For post-processing, Adobe Premiere Pro software was also used for data synchronization and preparation for advanced processing for other tasks, including a study of machine learning training methods for flashover detection.

4.1.1 Frame rates

The frame rate is the frequency at which a camera scans data and creates images. In general, a frequency lower than 9 Hz is reported to be inefficient and problematic for use on the fireground due to the lags [26]. However, the frame rate is unrelated to the thermal response time of a camera, and thus the frame rate does not indicate how quickly the device reacts to fast changes in the temperature/radiation in the field of view.

In the context of recording fire tests using both thermal cameras and regular vision cameras, the choice of a synchronous frame rate, in this case, 30 Hz, is crucial for several reasons. First, a consistent frame rate across all cameras[2] ensures that the data collected is temporally aligned, which is vital for accurately correlating visual and thermal data points. This alignment allows for a precise analysis of the fire's progression and characteristics, such as the spread of flames, heat distribution and the development of hot spots over time.

[2] For regular vision cameras, the framerate is 29.97 Hz.

Choosing a similar frame rate for all devices involved is necessary to maintain the integrity of synchronized playback and analysis. Discrepancies in frame rates can lead to asynchronous data, complicating the post-analysis process and potentially leading to inaccuracies in interpreting the dynamic behavior of the fire.

Furthermore, the selection of a 30 Hz frame rate strikes a balance between providing sufficient temporal resolution to capture fast-changing conditions and being manageable in terms of data storage and processing requirements. Higher frame rates, while offering more detailed temporal information, would significantly increase the volume of data generated, imposing greater demands on data storage and processing infrastructure. Conversely, lower frame rates might not adequately capture rapid transitions in fire behavior, which is critical for understanding and modeling fire dynamics. Therefore, the chosen frame rate of 30 Hz can be an optimal choice for ensuring detailed, accurate and manageable fire test data collection.

All the cameras recorded data synchronously at a framerate of 30 Hz, where possible. It should be noted that although in the software settings of all cameras, the framerate was set at 30 Hz, we found that the recorded data did not follow the initial settings in some of the tests. Table 4 shows the different frame rates of the recorded data by each camera. From the table, it can be seen that FLIR T650sc did not follow the initial settings of the data acquisition software tool, FLIR Research Studio. While it is still under investigation, the reason for this discrepancy between the settings and the recorded framerate could be the different specifications of the connectors and the two tower PCs used in the image data acquisition.

Table 4. Camera settings and output frame rates

Device	Data		Temperature range selected	Test 1	Test 2	Test 3	Test 4	Test 5	Test 6	Test 7
	Type	Format		Recorded frame rate (Hz)						
Canon camera	RGB video	*.MP4	n/a	29.97	29.97	29.97	29.97	29.97	29.97	29.97
SJ4000	RGB video	*.MOV	n/a	30.00	30.00	30.00	30.00	30.00	30.00	30.00
FLIR A8303sc	Raw Radiometric IR Video	*.ats	40˚C to 1200˚C	30.00	30.00	30.00	30.00	30.00	30.00	30.00
FLIR T650sc	Raw Radiometric IR Video	*.seq	100˚C to 650˚C	7.50	28.60	7.00	27.00	30.00	29.00	29.00
FLIR T650sc	Raw Radiometric IR Video	*.seq	300˚C to 2000˚C	7.50	28.60	7.00	27.00	30.00	29.00	29.00
FLIR K65	IR non-radiometric Video	*.mp4	0˚C to 650˚C	30.00	30.00	30.00	30.00	30.00	30.00	30.00

4.2 Image data analysis

A comparison between data recorded with the various cameras in Test #1 is illustrated in Figure 23.

4.2.1 Image data of smoke and flame development in a room fire

Based on our literature review of the field, to detect flashover occurrence from vision data, we can rely on a few indicators of flashover. These indicators are smoke and flame rolling out from the opening as well as observing hot and high-speed flame and gases toward the outside of the opening [16], [27], [28], [29], [30], [31], [32]. It means that from the figure, flashover indicators or features are more outside of the room fire test. Therefore, as a general conclusion, the usage of RGB cameras might be a better solution for the identification of flashover occurrences. Recently, we proved this idea in a research work [32]. The problem now is that the goal of many studies is not to detect flashover occurrence, the goal is to predict the flashover onset. In this case, to use vision-based technologies, it is vital to look at the trend of fire and smoke instead of indicators of flashover. Thermal IR cameras are therefore great candidates for this task. For the sake of simplification, we only illustrated data from Test #4. Data from other tests had a similar structure. For example, look at a few images from Test #5 in Figure 24.

4.2.2 Temperature range and sensitivity

By setting higher temperature ranges for the thermal IR cameras, lower temperature spans are lost. Conversely, by setting the camera temperature range for lower temperatures, the camera detector will be saturated near the range of flashover temperatures (i.e., 600–650°C). The dynamic range for almost all FLIR cameras is 14-bit, restricting the resolution of the camera to this 14-bit. Therefore, calibrating the camera for larger temperature ranges (e.g., from 40–1200° C) will decrease the temperature resolution and accuracy significantly. For this reason, IR cameras usually have overlapping temperature spans, and using super-resolution (i.e., IR cameras collect data by switching between several temperature spans and then merging them together digitally), it is possible to cover a larger range of temperatures. Employing super-resolution for this project was not successful since the only camera that has this feature (i.e., FLIR A8303sc) requires a ND2 filter to be used for high-temperature ranges, while for lower ranges, no filter is required. Details of using ND2 filters for FLIR cooled detector cameras can be found in [24].

Like any digital image, thermal images are composed of pixels. In thermal imaging, each pixel represents a specific temperature data point. These data points are assigned a unique color or

shade based on their value, such that as the thermal sensor detects changes in heat energy, it reflects these changes by adjusting the colour or shade of each pixel. To aid in the interpretation of these colours, a 'colour bar' is typically included alongside the thermal image. This colour bar serves as a key, mapping specific colors to their corresponding temperature values. It provides a visual scale that helps viewers understand the temperature range represented within the image, from cooler areas depicted in darker shades or cooler colors, to hotter regions shown in lighter shades or warmer colors. By referencing the color bar, users can accurately gauge the thermal variations captured in the image, making it an essential tool for analysis in applications ranging from industrial inspection to medical diagnostics.

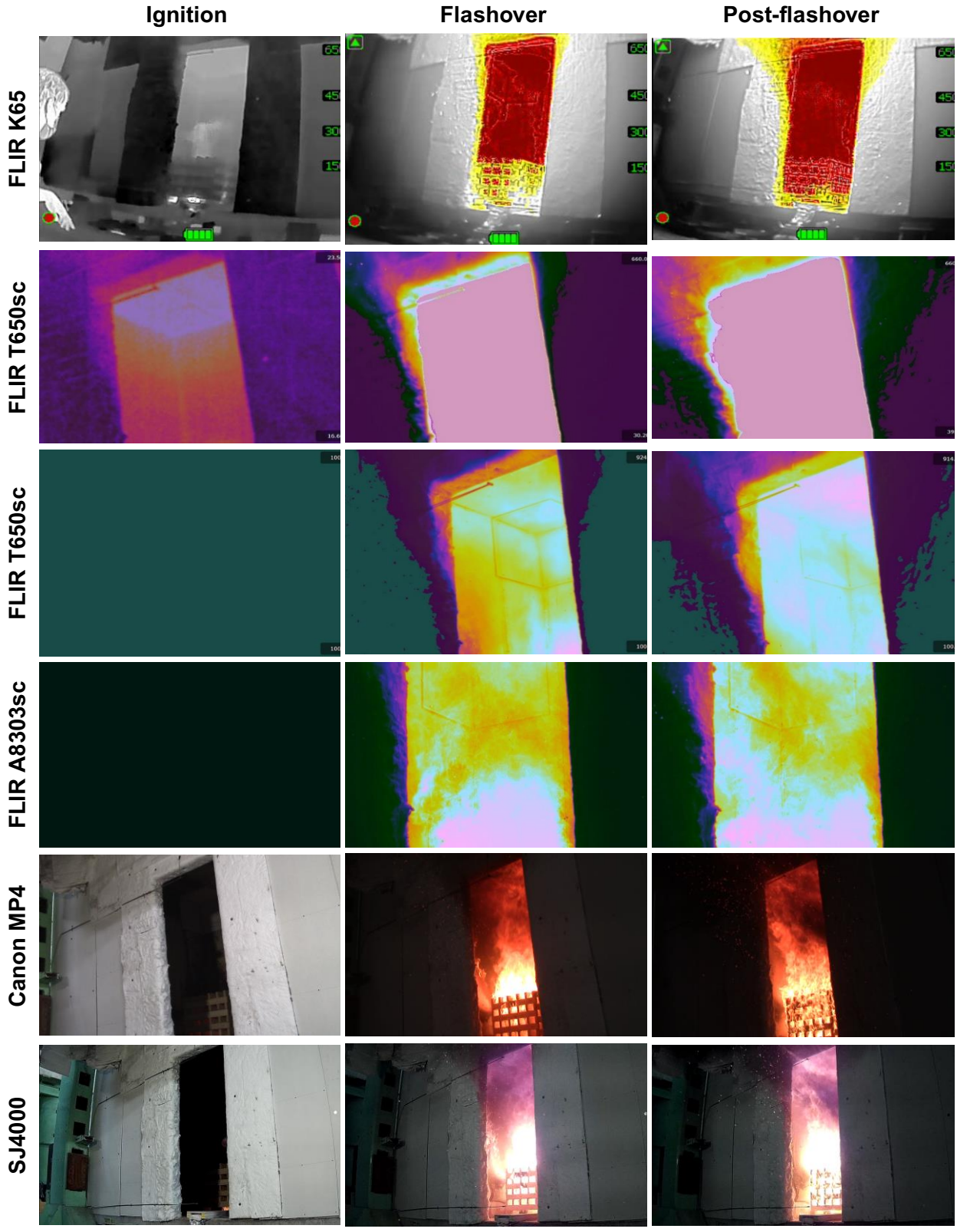

Figure 23. A comparison table between data recorded by RGB and IR camera in Test # 1 for three critical times, including flashover

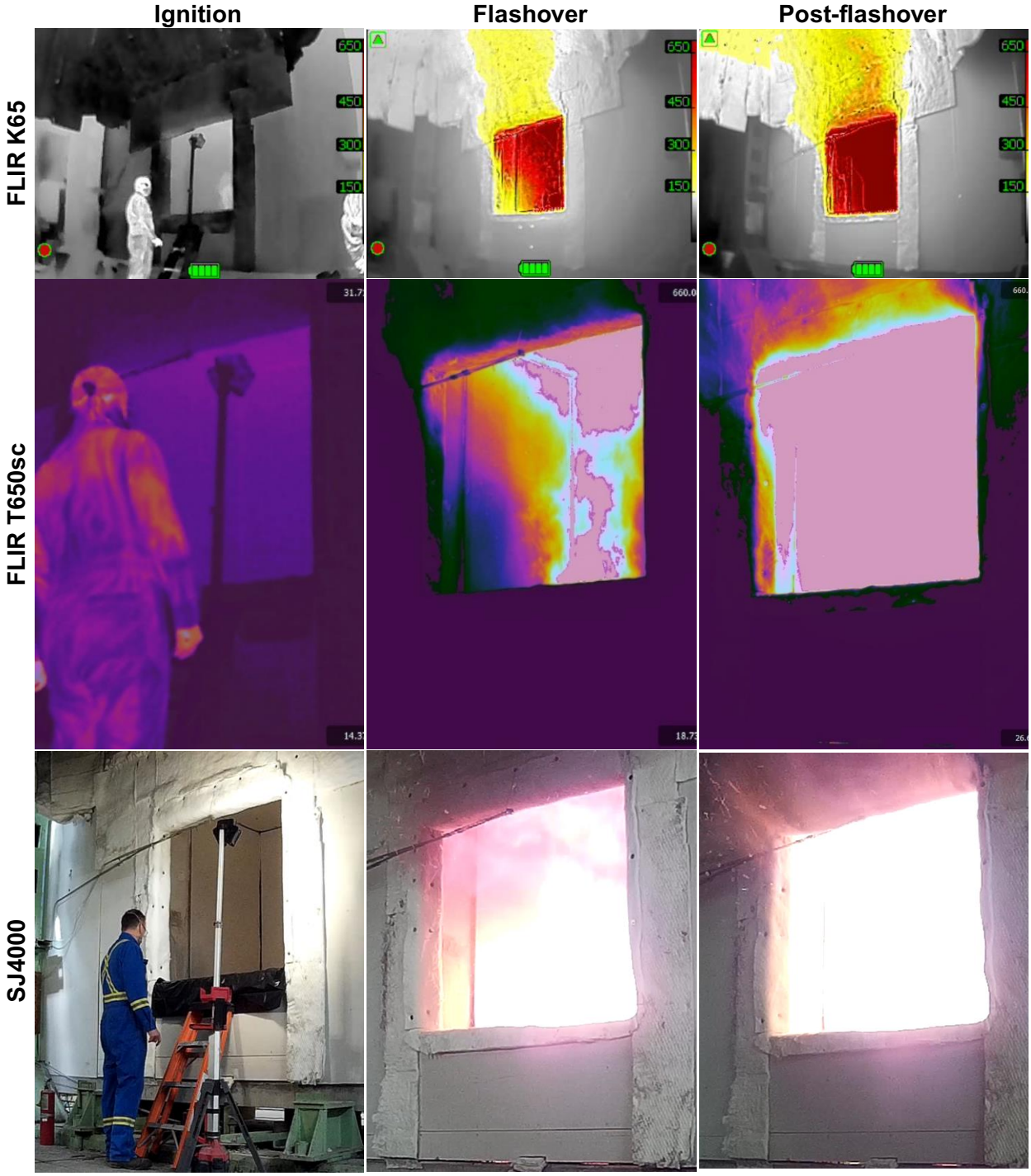

Figure 24. A comparison table between data recorded by some of RGB and IR cameras in Test # 4 for three critical times, including flashover

4.2.4 Temperature reading by IR cameras

The calibration accuracy of thermal IR cameras has been investigated in [24]. From that experimental report, using blackbody with different temperature values, the accuracy of all cameras is acceptable and within the standard range (±2%).

Figure 25 is an example of a comparison between the same frame captured by three main thermal IR cameras in Test #1. From the figure, in the time of flashover, which is calculated from the sensor's data (HRR, HF and thermocouples), the average temperature values for each camera are different. FLIR A8303sc shows an average value of ~830°C for the smoke region. The FLIR T650sc with a temperature range of 2000°C shows ~772°C while the same camera with a temperature range of 650°C reached its saturated region, which is 650°C. Therefore, from this comparison, we can see it is crucial to consider that what appears to be the "same" point in images from different cameras might not actually represent the same physical point, due to variations in camera angles and focal points. Additionally, the difference in wavelength sensitivity between the MWIR A8303sc camera and the LWIR T650sc camera suggests that the A8303sc is more likely to "see through" smoke and thus report the temperature behind the smoke layer, while the T650sc more likely reports the temperature of the smoke layer itself. These technical nuances underscore the need for further investigation to interpret these variations accurately. Therefore, we compare visual differences qualitatively between data recorded by all cameras in the following. Differences in temperature readings by all cameras were explored, as shown in Figure 27, details of which are discussed in the calibration report [24]. This discrepancy in temperature needs to be further studied.

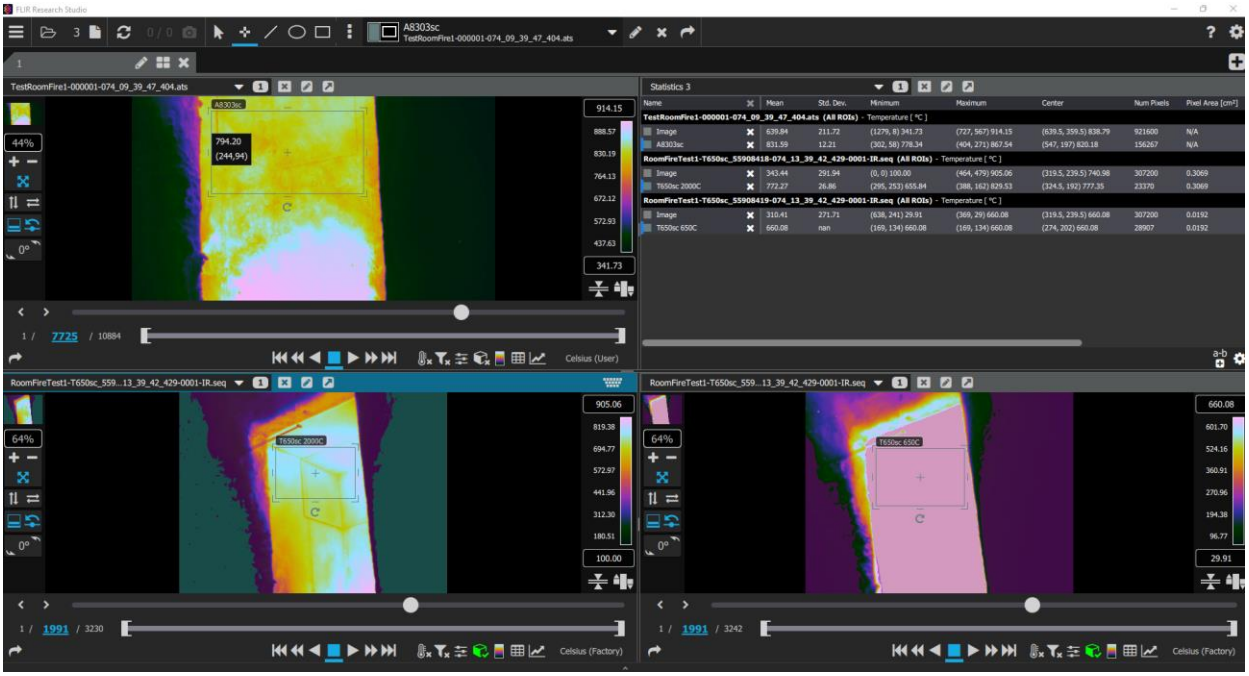

Figure 25. Sample comparison of flashover onset in test 1 for three main thermal IR cameras

The calibration accuracy of FLIR IR cameras has been investigated in the calibration report of this project [24]. However, here, we only evaluated one other sample to see the difference between the temperature accuracy of the temperature sensor installed in 2.4 m between wood cribs with FLIR A8303sc camera. Figure 26 shows one sample image from Test #5 with a selected region of interest (ROI) around the sensor at a height of 2.4 m. The tip of the sensor can be seen clearly in the figure. Two graphs related to the same video data have been shown in Figure 26 as well, calculated by averaging temperature values in the vertical axis of the selected ROI for one slide (i.e., the image in Figure 26) and for the whole recorded data (i.e., temporal graph).

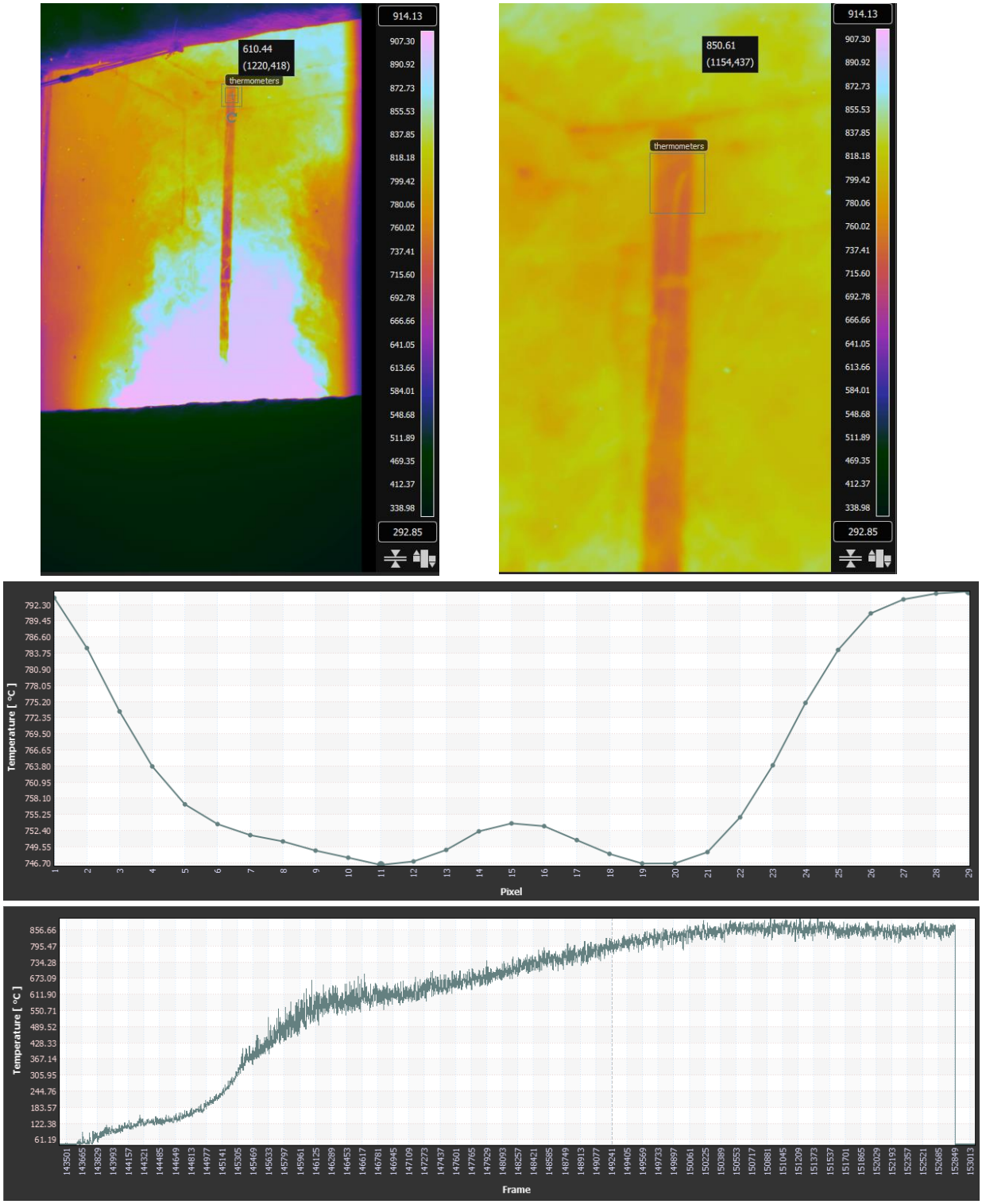

Figure 26. One example of analysis of temperature accuracy for the FLIR A8303sc camera. The top image was captured from Test #5 around flashover occurrence. The zooming image shows the thermocouple clearly in around 2.4 m above the ground. Two graphs in the bottom show the vertical average temperature of ROI in one image and in the whole video (temporal).

By exporting temperature trend data in Figure 26 (bottom graph) and plot in parallel with sensor data in Test #5 (the whole sensor's data can be found in Figure 20), we could compare temperature data between the sensor and average temperature calculated from the ROI of the IR data in Test #5 recorded by FLIR A8303sc. **Error! Reference source not found.** shows this c omparison result. From the figure, it is clear that the temperature trend in both technologies is similar. Of course, the temperature data from the IR camera is noisier due to averaging, measurement uncertainty, smoke movements in front of the camera and inaccurate calculations in the camera due to unknown parameters such as emissivity, distance, humidity and many other factors.

With all these caveats, this experiment shows that thermal IR can still be utilized as a reliable non-invasive technique to monitor temperature growth in fire incidents. If we consider sharp temperature growth as an early indication of flashover, then by monitoring temperature by thermal infrared cameras, we can predict flashover with a high degree of confidence. Preliminary scientific investigation of using thermal IR cameras for flashover prediction and detection can be found in a recent publication [33].

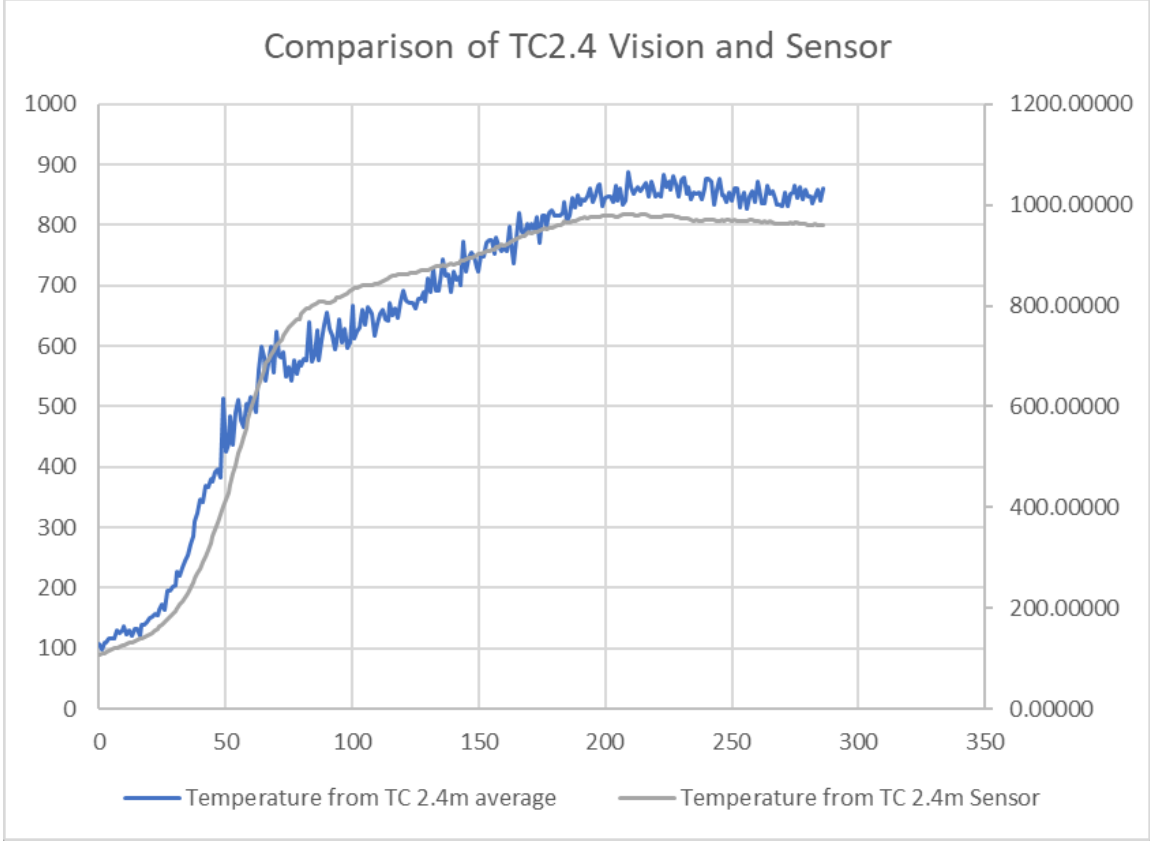

Figure 27. Result of comparison between temperature calculation from the vision IR camera (FLIR A8303sc) and thermocouple installed in the test room at a height of 2.4 m in the same test experiment (Test #5)

4.2.5 Acoustic image sensor response to a room fire

An acoustic imaging camera (FLIR si124) was explored for potential applications to fire-related information collection. The ultrasonic and vision-based detection camera is usually used for locating pressurized leaks in compressed air systems or detecting partial discharges from high-voltage electrical systems [25]. For the first time, we used this acoustic imaging camera to record data on flashover phenomena. This device has 124 microphones to locate the source of noise in the environment. Figure 28 shows this new technology used in our room fire test experiments.

While this camera is designed to find electric noises and pressurized leaks, it also shows the potential to locate a fire. Figure 28 shows the image captured in Test #4 by FLIR si124 acoustic imaging device. Before ignition, the device detected an electric box in our lab. After the fire ignited, the camera only spotted the fire. This proves that fires emit combustion products and heat in conjunction with electrical signals. Note that there were many other sources of electrical noise in the test area, yet the device identified the flame as the most significant electrical noise source. Also, we experimented with a device that was able to sense the noise caused by fire, which is an interesting feature of the device and could be utilized for fire detection in complex buildings.

While further investigation is necessary to fully understand the responses of the ultrasonic detection device to fires, our exploration shows clearly that fires emit acoustic/electrical signals, and this feature could be used in detecting fire, and possibly in suppressing fires.

Before ignition

After ignition

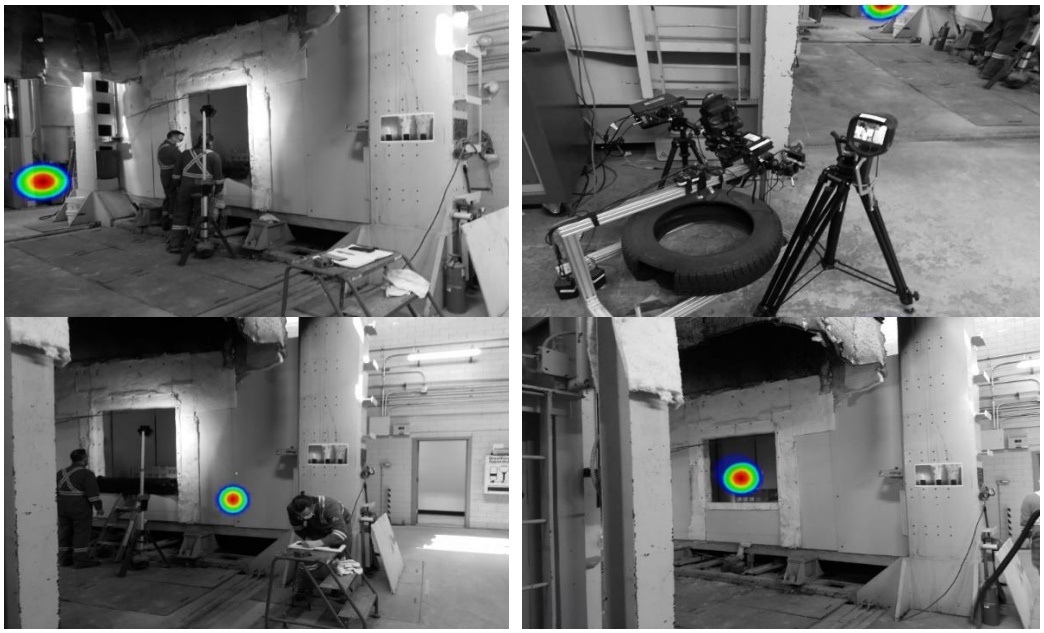

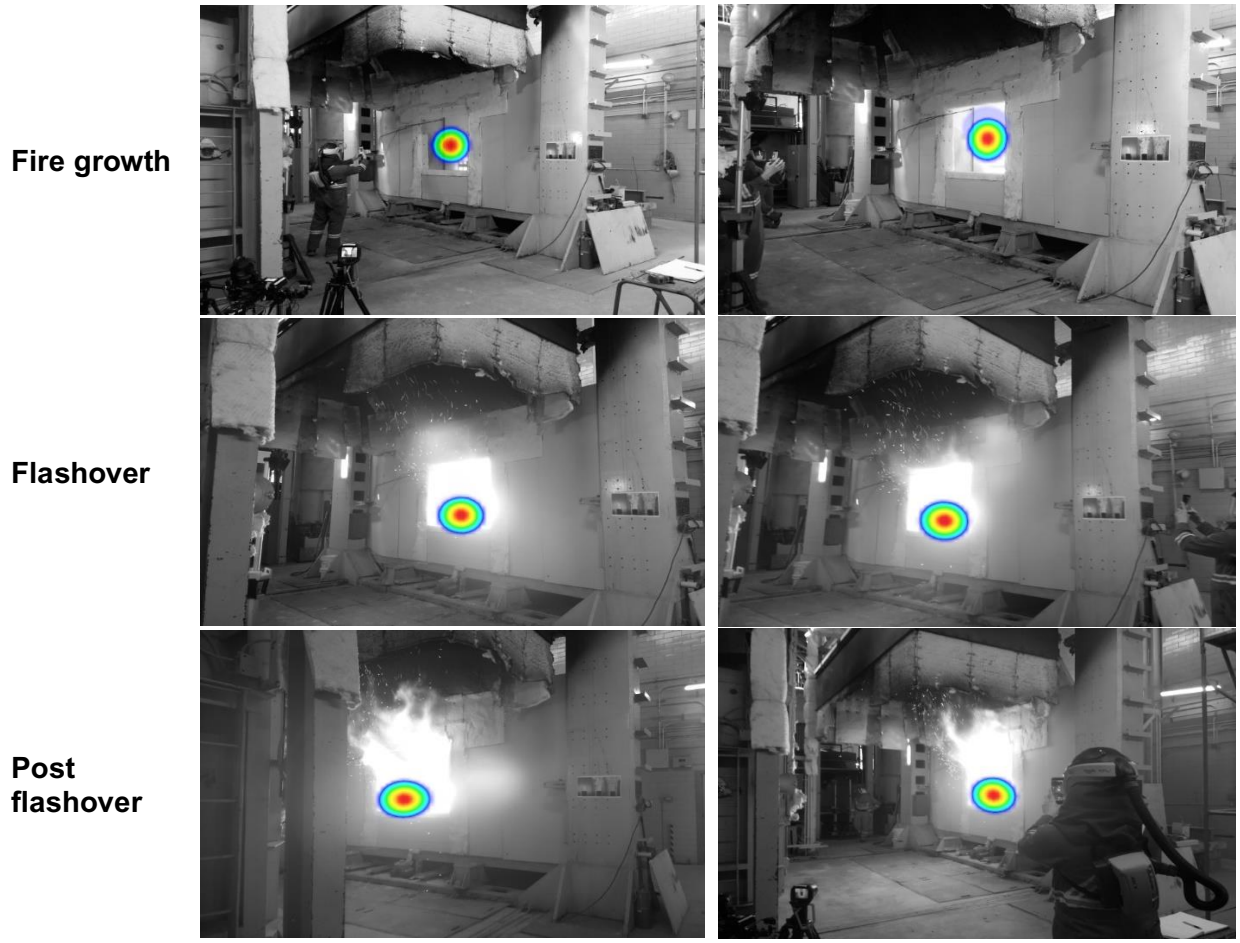

Figure 28. Sample image data recorded by FLIR si124 acoustic imaging camera in Test #4

5 Summary and conclusion

This report presents a complete explanation of seven full-scale room fire experiments conducted at the Fire Safety Unit, National Research Council Canada. The project is one phase of a bigger project, called Vision-based Smart Firefighting Tool Development (VSFTD). The main goal of the project was to address the needs of the project, specifically:

- Address the lack of realistic and full-scale room fire experiments containing flashover phenomena.
- Provide the possibility of recording various types of data to aid the development of machine learning and computer vision detection, and the prediction of flashover phenomena.
- Allow researchers to study room fires with different room configurations in terms of opening, door size and fuel amounts.
- Methods for analysis.

- Compare imaging and sensing technologies to understand each one's performance in monitoring, detecting and predicting flashover.
- Provide the same angle of view for recording vision-based data for comparison and mapping from one imaging technology to another.
- Validate vision-based methods and imaging technologies using data recorded simultaneously by fire-resistant sensors.
- Analyze the accuracy of in-house calibrations of mid-wave IR cameras for fire temperature ranges.

Because the main goal here is to study the flashover phenomenon, it is worth defining flashover. The latest tenable hazard criterion for occupants and firefighters is flashover, the most serious and fatal event in room fire incidents. Flashover onset in an enclosure is defined as a rapid transition in the state of the fire, whereby total surfaces of combustible materials start to burn simultaneously, and the flame spreads throughout the entire room. The main reason for flashover in a confined fire is that the hot smoke layer accumulated near the ceiling rapidly heats the exposed surface of all the items in the room. Subsequently, the temperature rise in the surface of combustible contents produces hot pyrolysis gases that are ignited along with the bottom of the ceiling layer. In order to train AI/ML to detect and predict this fire phenomenon, we need to provide a large number of samples. The result of this project report and our comprehensive database recorded for the first time from actual size room fires using various imagery devices and other common sensors can be used in the future for training and validating advanced AI models for the purpose of flashover detection and prediction.

6 References

[1] M. H. Mozaffari, Y. Li and Y. Ko, “Real-time detection and forecast of flashovers by the visual room fire features using deep convolutional neural networks,” *Journal of Building Engineering*, vol. 64, p. 105674, 2023.

[2] M. H. Mozaffari, Y. Li, Y. Ko, M. H. Mozaffari, Y. Li and Y Ko, “Generative AI for Fire Safety,” *Applications of Generative AI*, pp. 577–600, 2024, doi: 10.1007/978-3-031-46238-2_29.

[3] Y. Ko, M. Hamed Mozaffari and Y. Li, “Fire and Smoke Image Recognition,” pp. 305–333, 2024, doi: 10.1007/978-3-031-48161-1_13.

[4] H. Mozaffari, Y. Li and Y. Ko, “Real-Time Assistance to Firefighters Using Convolutional Neural Networks,” *Celebrating the Success of Women in STEM Symposium: Pushing the frontiers of research through collaboration*, no. 2014, p. 2016, 2022.

[5] "ISO 13943:2023(en), Fire safety — Vocabulary." Accessed: Aug. 5, 2024. [Online]. Available: https://www.iso.org/obp/ui/#iso:std:iso:13943:ed-4:v1:en

[6] D. Drysdale, "The flashover phenomenon," *Fire Engineers Journal*, vol. 56, no. 185, pp. 18–23, 1996.

[7] A. C. Y. Y. Yuen, G. H. Yeoh, R. Alexander and M. Cook, "Fire scene reconstruction of a furnished compartment room in a house fire," *Case Studies in Fire Safety*, vol. 1, no. 1, pp. 29–35, 2014, doi: 10.1016/j.csfs.2014.01.001.

[8] V. Babrauskas, "Upholstered furniture room fires—measurements, comparison with furniture calorimeter data, and flashover predictions," *J Fire Sci*, vol. 2, no. 1, pp. 5–19, Jan. 1984, doi: 10.1177/073490418400200103.

[9] H. J. Kim and D. G. Lilley, "Flashover: A study of parameter effects on time to reach flashover conditions," *J Propuls Power*, vol. 18, no. 3, pp. 669–673, 2002, doi: 10.2514/2.5982.

[10] B. J. McCaffrey, J. G. Quintiere and M. F. Harkleroad, "Estimating room temperatures and the likelihood of flashover using fire test data correlations," *Fire Technol*, vol. 17, no. 2, pp. 98–119, 1981.

[11] M. C. Bruns, "Estimating the flashover probability of residential fires using Monte Carlo simulations of the MQH correlation," *Fire Technol*, vol. 54, no. 1, pp. 187–210, 2018, doi: 10.1007/s10694-017-0680-0.

[12] F. R. Centeno, M. Beshir and D. Rush, "Influence of wind on the onset of flashover within small-scale compartments with thermally-thin and thermally-thick boundaries," *Fire Saf J*, vol. 117, no. August, p. 103211, 2020, doi: 10.1016/j.firesaf.2020.103211.

[13] M. Beshir, Y. Wang, F. Centeno, R. Hadden, S. Welch and D. Rush, "Semi-empirical model for estimating the heat release rate required for flashover in compartments with thermally-thin boundaries and ultra-fast fires," *Fire Saf J*, vol. 120, p. 103124, Mar. 2021, doi: 10.1016/j.firesaf.2020.103124.

[14] S. Lee and K. Harada, "A simplified formula for occurrence of flashover and corresponding heat release rate," *Procedia Eng*, vol. 62, pp. 292–300, 2013, doi: 10.1016/j.proeng.2013.08.067.

[15] R. D. Peacock, P. A. Reneke, R. W. Bukowski, V. Babrauskas, R. D. Peacock and P. A. Reneke, "Defining flashover for fire hazard calculations," *Fire Saf J*, vol. 32, no. 4, pp. 331–345, 1999, doi: 10.1016/S0379-7112(03)00027-4.

[16] D. Cortés, D. Gil, J. Azorín, F. Vandecasteele and S. Verstockt, "A review of modelling and simulation methods for flashover prediction in confined space fires," *Applied Sciences*, vol. 10, no. 16, p. 5609, 2020.

[17] J. Francis and A. P. Chen, “Observable characteristics of flashover,” *Fire Saf J*, vol. 51, pp. 42–52, 2012.

[18] C.-C. Lin and L. L. Wang, “Real-time forecasting of building fire growth and smoke transport via ensemble kalman filter,” *Fire Technol*, vol. 53, no. 3, pp. 1101–1121, 2017.

[19] T. Zhang, Z. Wang, H. Y. Wong, W. C. Tam, X. Huang and F. Xiao, “Real-time forecast of compartment fire and flashover based on deep learning,” *Fire Saf J*, vol. 130, p. 103579, 2022.

[20] Z. Wang, T. Zhang, X. Wu, and X. Huang, “Predicting transient building fire based on external smoke images and deep learning,” *Journal of Building Engineering*, vol. 47, no. September 2021, p. 103823, 2022, doi: 10.1016/j.jobe.2021.103823.

[21] “ISO 9705-1:2016 - Reaction to fire tests — Room corner test for wall and ceiling lining products — Part 1: Test method for a small room configuration.” Accessed: Aug. 5, 2024. [Online]. Available: https://www.iso.org/standard/59895.html

[22] V. Babrauskas, “Estimating room flashover potential,” *Fire Technol*, vol. 16, no. 2, pp. 94–103, 1980.

[23] P. H. Thomas, “Testing products and materials for their contribution to flashover in rooms,” *Fire Mater*, vol. 5, no. 3, pp. 103–111, 1981.

[24] M. H. Mozaffari, Y. Li, Y. Ko and M. Weinfurter, “User calibration of a mid-wave infrared camera for fire research,” p. 66, 2023.

[25] S. Dudić, I. Ignjatović, D. Šešlija, V. Blagojević, and M. Stojiljković, “Leakage quantification of compressed air using ultrasound and infrared thermography,” *Measurement*, vol. 45, no. 7, pp. 1689–1694, Aug. 2012, doi: 10.1016/J.MEASUREMENT.2012.04.019.

[26] A. S., “Thermal Imaging Cameras in the Fire Service: Asset or Detriment? You Decide,” Fire Apparatus & Emergency Equipment Staff.

[27] K. Yun, J. Bustos and T. Lu, “Predicting rapid fire growth (flashover) using conditional generative adversarial networks,” *IS and T International Symposium on Electronic Imaging Science and Technology*, vol. 2018, no. 9, pp. 2751–2757, 2018, doi: 10.2352/ISSN.2470-1173.2018.09.SRV-127.

[28] Y. Li and Y. Ko, “Development of a hybrid algorithm to predict room fire flashovers based on vision data,” 2021. doi: https://doi.org/10.4224/40002684.

[29] Y. Li and Y. Ko, “Vision-based smart firefighting tools to predict room fire flashovers,” *Nrc Techx 2022*, p. 2021, 2022.

[30] A. L. Huyen *et al.*, “Dynamic fire and smoke detection and classification for flashover prediction,” *Pattern Recognition and Tracking XXXII*, vol. 1173502, no. April, p. 1, 2021, doi: 10.1117/12.2588175.

[31] A. Dexters, R. R. Leisted, R. Van Coile, S. Welch and G. Jomaas, “Testing for knowledge: Application of machine learning techniques for prediction of flashover in a 1/5 scale ISO 13784-1 enclosure,” *Fire Mater*, vol. 45, no. 6, pp. 708–719, 2021, doi: 10.1002/fam.2876.

[32] M. H. Mozaffari, Y. Li and Y. Ko, “FlashoverNet: Vision-based Flashover Detection and Prediction in Room Fire Incidents using Deep Convolutional Neural Networks,” pp. 1–2.

[33] H. Mozaffari *et al.*, “Detecting Flashover in a Room Fire based on the Sequence of Thermal Infrared Images using Convolutional Neural Networks,” *Canadian AI 2022*, May 2022.

Appendix A - flashover correlations

There are two types of flashover correlations used in the experiments: Babrauskas [22] and Thomas [23].

A.1 Babrauskas' correlation

Babrauskas' correlation [22] is given as:

$$\dot{Q}_{FO} = 750 A_0 \sqrt{H_0}$$

Where $\dot{Q}_{FO}$ (kW) is the heat release rate that will cause flashover to occur, A_0 (m^2) is the area of a ventilation opening, and H_0 (m) is the height of the ventilation opening.

A.2 Thomas' correlation

Thomas' correlation [23] is given as:

$$\dot{Q}_{FO} = 7.8 A_T + 378 A_0 \sqrt{H_0}$$

Where A_T (m^2) is the total internal area of bounding surfaces of an enclosure.

Appendix B - Calculation of measured $\dot{Q}_{FO}$

The calculation of measured QFO is based on:

$$\dot{Q}_{FO} = [E - (E_{CO} - E)\frac{(1-\phi)}{2\phi}\frac{X_{CO}^{Ae}}{X_{O_2}^{Ae}}]\phi \frac{\dot{m}_e}{1+\phi(\alpha-1)}\frac{M_{O_2}}{M_a}(1 - X_{H_2O}^{o})X_{O_2}^{A^o}$$

Where E is the defined heat release per mass oxygen consumed, E_{CO} is the difference in heat released by CO and CO_2 (283 kJ/mol of oxygen consumed). α is the expansion factor due to chemical reactions. M_{O_2} and M_a are the defined molecular weights of O_2 and air, respectively. $X_{H_2O}^{o}$ is the mol fraction of water vapour.